JUNE 2001
VOL. 11, NO. 2

SPIE's International Technical Group Newsletter

ELECTRONIC IMAGING

A psychophysically-based model of glossy surface appearance

Color and gloss are two fundamental attributes used to describe surface appearance. Color is related to a surface's spectral reflectance properties. Gloss is a function of its directional reflectance properties. Many models have been developed for describing color, from simple RGB, to the more sophisticated Munsell, XYZ, and CIELAB models that have grown out of the science of *colorimetry*. Colorimetric models make it easier to describe and control color because they are grounded in the psychophysics of color perception. Unfortunately similar psychophysically-based models of gloss have not been available.

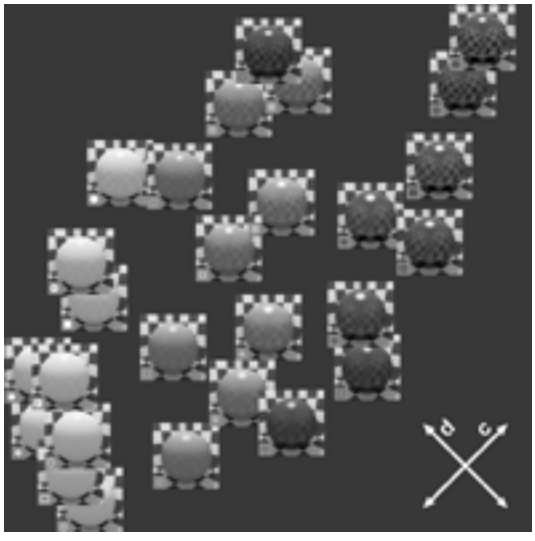

Figure 1. Visual gloss space with its (c) contrast and (d) distinctness dimensions.

We have developed a new model of glossy surface appearance that is based on psychophysical studies of gloss perception.[1,2] In two experiments, we have used multidimensional scaling to reveal the dimensionality of gloss perception and to find perceptually meaningful axes in visual gloss space, and used magnitude estimation to place metrics on these axes and predict just noticeable differences in gloss. Stimuli for the experiments were generated using physically-based image synthesis techniques. Our test environment consisted of a painted sphere enclosed in a checkerboard box illuminated by an overhead area light source. Images were rendered with a Monte Carlo path-tracer incorporating an isotropic version of the Ward light reflection model:

$$\rho(\theta_i,\phi_i,\theta_o,\phi_o) = \frac{\rho_d}{\pi} + \rho_s \cdot \frac{\exp[-\tan^2\delta/\alpha^2]}{4\pi\alpha^2\sqrt{\cos\theta_i\cos\theta_o}}$$

where $r(\theta_i,\phi_i,\theta_o,\phi_o)$ is the surface's bi-directional reflectance distribution function (BRDF) that describes how light is scattered by the surface. In addition to angular dependencies (θ,ϕ,δ), the Ward model uses three parameters to describe the BRDF: ρ_d, the surface's diffuse reflectance; ρ_s, the energy of the specular lobe, and α, the spread of the specular lobe. By setting each parameter to three levels we generated the 27 stimulus images shown in Figure 1.

In the first experiment, subjects viewed pairs of images and judged how different they appeared in gloss. We analyzed these gloss difference judgments with multidimensional scaling to recover the visual gloss space

continued on p. 8

Calendar *—See page 10*

Technical Group Reg Form *—See page 11*

NEWSLETTER NOW AVAILABLE ON-LINE

Technical Group members are being offered the option of receiving the Electronic Imaging Newsletter in an electronic format. An e-mail notice is being sent to all group members advising you of the web site location for this issue and asking you to choose between the electronic or printed version for future issues. If you have not yet received this e-mail message, then SPIE does not have your correct e-mail address in our database. To receive future issues of this newsletter in the electronic format please send your e-mail address to spie-membership@spie.org with the word EI in the subject line of the message and the words "Electronic version" in the body of the message.

If you prefer to continue to receive the newsletter in the printed format, but want to send your correct e-mail address for our database, include the words "Print version preferred" in the body of your message.

Circular dynamic stereo system

The automatic inference of depth information has been one of primary aims of computer vision. Stereo-vision and slit-ray-projection methods are often used to achieve this, but there are difficulties in implementing these systems. In a stereo vision system, for example, computer algorithms designed to find matching features in pairs of frames can have problems when several matches are possible. In implementing the slit-ray-projection method, on the other hand, the target must be stationary during the measurement.

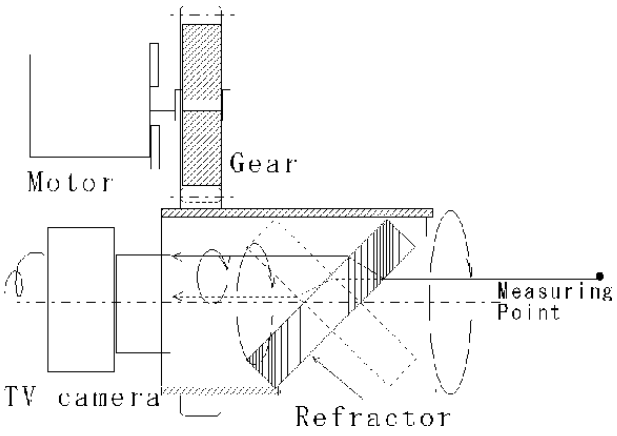

Figure 1. Circular dynamic stereo system.

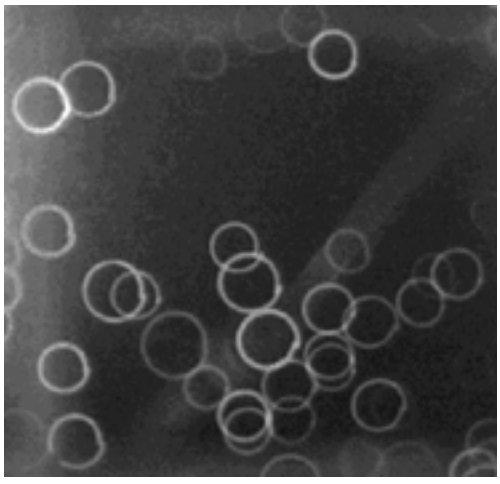

Figure 2. Tracer particle with circular shift.

In order to cope with these problems, we have developed a circular dynamic stereo system[1,2] that uses a single TV camera. This camera moves sideways with respect to measuring points on the object. As a result, the amount of displacement undergone by its image on the image plane is directly proportional to the displacement of the camera and inversely proportional to the measuring point's distance from it. The distance between camera and measuring point can therefore be estimated using these two parameters. This method is well known, and has been used in monocular motion stereo systems (MMSS). However, our circular dynamic stereo system realizes this MMSS in compact setup and enables the measurement of moving targets. A simplified setup of our system is shown in Figure 1. By introducing a refractor on the camera lens, the image of the measuring point undergoes a displacement on the image plane that is related to the distance between the TV camera and the measuring point. That is, the displacement r on the image is inversely proportional to the distance D between the measuring point and the camera as,

$$D = \frac{f \cdot d}{r} \qquad (1)$$

where f is the focal length of the camera and d is the magnitude of shift caused by refractor. When the refractor is rotated at high speed (3600rpm) during the TV camera exposure, circular streaks appear on the image due to the rotational shift. Since the size of the circular streak is inversely proportional to the distance of the measuring point from the camera, each streak contains 3D information about a measuring point, and this information can be extracted by processing the streak image.

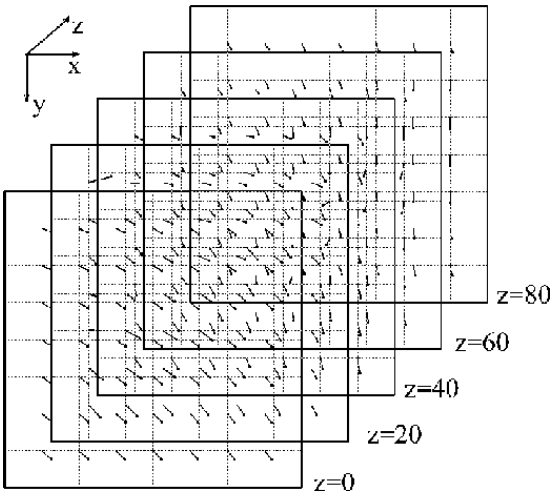

Figure 3. Velocity distribution in a water tank.

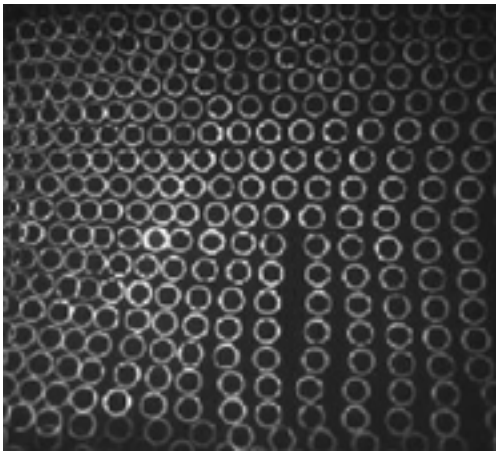

Figure 4. Multiple laser spots with circular shift.

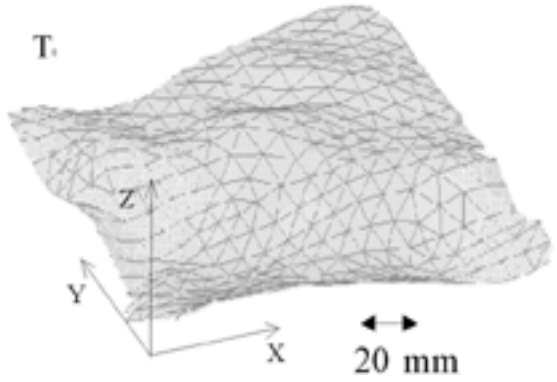

Figure 5. Reconstructed water surface.

What follows are a few examples to the feasibility of circular dynamic stereo system. The first is the measurement of 3D velocity distribution in a water tank. Tracer particles are introduced into the water and these particles to move with water flow. The velocity distribution of the water can then be obtained by measuring the movement of tracer particles. Figure 2 shows an image of streaks of tracer particles recorded by the circular dynamic stereo system: bigger streaks correspond to the particles closer to the TV camera and smaller streaks those

continued on p. 9

Human color constancy: model and performance

Color constancy (CC) is a psychophysical phenomenon in which a system is partially able to discount the chromaticity of the illumination. For example, a page of a book appears white to a human reader both indoors under a yellowish light, and outdoors under the bluish daylight. This results from the fact that the perceived color of an object is not just a simple function of the spectral composition of the light reflected from it, but it also depends on the spatial distribution of other chromatic stimuli in the field of view. A camera does not posses this ability, therefore color corrections of images are necessary.

Although the issue of CC has been investigated for more than a century, there is still no widely accepted model that explains or imitates the human CC capability. However, our new CC biological model[1] succeeds in correcting the color of images in a similar way to the visual system. It performs automatic color correction of still images and video sequences under single and multiple illumination conditions. This algorithm takes advantage of retinal mechanisms of adaptation (gain controls).

Most of the CC algorithms that have been applied to real images so far were not intended to imitate human visual physiology and performance, as this algorithm is, but rather for exactly extracting reflectances and illuminations. These machine vision algorithms are better suited to applications such as color object identification and, in addition, none were intended for video image applications (i.e. none include human dynamical adaptation mechanisms).

Model

The model (Figure 1) describes the transformation of visual stimuli to the responses of three types of color-coded on-center Retinal Ganglion Cells (RGCs)—the last chain of data processing in the retina—and the transformation of these responses to a perceived image. These cells have a color-opponent receptive field (RF) with a center-surround spatial structure. (An RF is that region in the visual field that elicits a cell response.) The RGC's center and surround regions adapt separately, each by two mechanisms of local and remote adaptation. Local adaptation refers to that occurring in the RF's regions (center or surround) owing to their own inputs, whereas remote adaptation refers to the effect of more peripheral regions. Only then are the two RF regions subtracted (through a "difference of Gaussians").

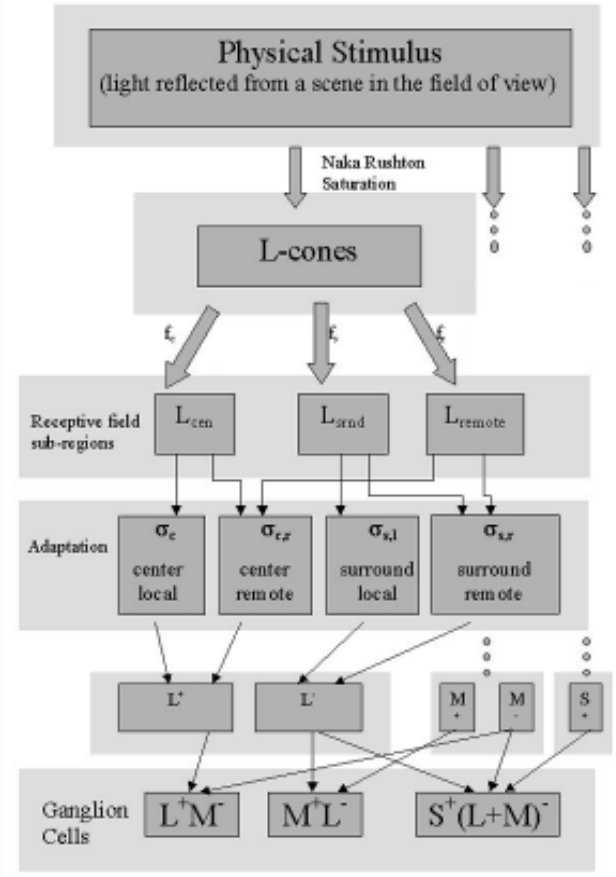

Figure 1. Schematic of color constancy algorithm.

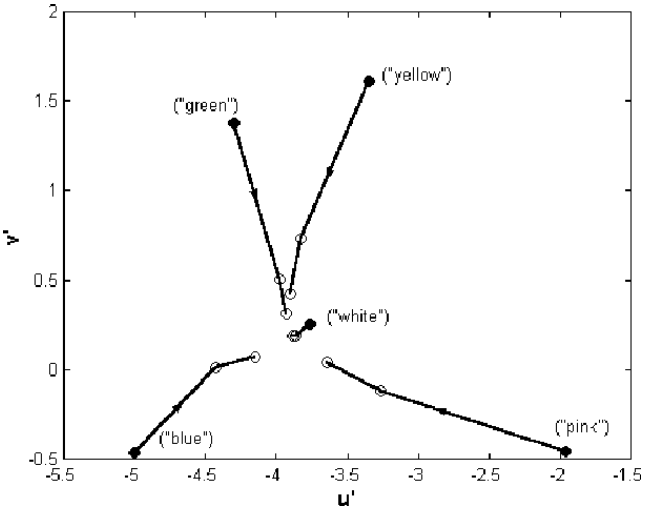

Figure 2. Color coordinates of an achromatic reference patch under different illuminations, and their shift as a result of algorithm corrections.

For moving (video) images, the adaptation functions implement a "curve-shifting" operation[1] and include a dynamic time-filter: the time constant of which depends on the temporal history of the stimuli. In single (still) images, where the responses have already reached a steady state, the model generates a corrected image by transforming the simulated RGCs' responses (at any location in the retina) into a perceived color. To do this, it uses a mathematical inverse function.

Performance

To evaluate the performance of the model, we calculated two indices: a human perception index (HPI) and a machine vision index (MVI). Both are based on distances between images: the average distance between the color coordinates of pairs of corresponding pixels in Lu*v* space. The human perception index (HPI) measures the distance that is formed between two perceived (corrected) images due to chromatic illumination. Thus, the index refers to the distances between two output images of the algorithm. One is an image taken under chromatic illumination, and the other is the same scene, taken under a reference achromatic illumination. The machine-vision index (MVI) compares a corrected chromatic illumination image to an achromatic illuminated reference image. Thus, the MVI measures to what extent the corrected image represents the spectral reflectance properties of surfaces in the scene

Calculations yielded positive values for both indices (indicating improved CC) for a large repertoire of images taken under different chromatic illuminations, both single and multiple.

To further quantitatively evaluate the degree of CC correction achieved by the algorithm, the u*v* color coordinates of a reference grey square patch were calculated for different images of the same scene taken under different illuminations: pink, yellow, green and blue (Figure 2, solid circles). Arrows show the progress from the original "colored" image, through a mild correction, to a stronger correction (open circles). In addition, Figure 2 includes the coordinates of the reference patch in a reference image, taken under achromatic (white) illumination, and those of this reference patch after the reference image was subjected to algorithm corrections under the same conditions (open circles). Arrows progression indicates a shift from the illuminant's

continued on p. 8

Soft computing methods for the segmention of human brain images

The field of image-processing based on distributed and parallel computing is becoming more and more important for many different applications. Medical applications, especially in radiology, benefit from many methods of image processing.[1,2] But, in contrast to industrial applications where the same structures have almost the same appearance, most medical structures greatly differ in the way they look. Beside "classical uncertainties" like noisy data or smooth transitions between single structures, often the so-called inter-individual variability increases the difficulty of identifying segmented structures. Each MRT-data set of a (healthy) human head contains the same structures but with different features like location, form, size, brightness, etc..[1,2] The variability of these structures can be handled with different methods. We use "fuzzy object descriptions to describe size, roundness, orientation, homogeneity and other features. We also use more general models such as: Fuzzy Object Models (FOMs)".[1]

An iconic fuzzy set,[3,4] introduced by Rosenfeld as a fuzzy image subset, is: "A figurative representation of a fuzzy set where each pixel represents a numerical measure of uncertainty. Both methods of using fuzzy descriptions and iconic fuzzy sets are introduced in order to obtain a similarity-measure for the comparison of stored anatomical model descriptions (linguistic and figurative) with segmented structures and their features."[2] The representation using iconic fuzzy sets instead of linguistic descriptions allows an easier way to describe some medical structures, and can be seen as a supplemental method for classification. This results from several knowledge acquisition sessions with medical experts. Often, they describe some structures with a sketch or a comparison ("this object looks like a ...") to complement their linguistic description. Each proposition in the following text describes the two-dimensional case: an extension to the three-dimensional can be done using mainly simple adaptations.

Segmentation of images means the partitioning of interesting objects from background. In the task of brain segmentation, the interesting object is the brain and its integral structures such as the brain stem, corpus callosum or cerebellum. First of all, the region of interest with a gross brain segmentation can be determined by a neural network. Beside this ROI-detection, some low-level knowledge about features of the brain and its structures are used for a fuzzy-region growing method and the selection of the seed points (starting pixel for the region growing). This knowledge is used for fuzzy filters like $F_{position}$ and $F_{brightness}$ shown in the following equations.[2]

$$F_{position} = \tau\left(\mu_{V_{2D}}, \mu_{H_{2D}}\right)$$

$$F_{brightness} = \mu_B(I)$$

V2D and H2D describe the vertical and horizontal restriction of the point-positions, τ is a arbitrary t-norm and I represent an image and μ is the membership function. The pixels in the resulting picture have different grey values, which represent the measure of confidence to be a useful seed point. Every pixel is selected as a seed point and the region growing process starts. Then each added pixel gets a measure of confidence that is not larger than the measure of the corresponding seed point or the neighboring pixel. It should be pointed out that the resulting structures are iconic fuzzy sets with pixels of different confidences to be the correct (searched for) structure. The next step of classification is not easy, because each found structure (there are several hundred) has to be divided into its α-cuts, and then their classification attempted. So the segmentation process delivers few correct divided structures and works on a very low level of pixel aggregation. The region-growing methods, however, produces convex iconic fuzzy sets, so it is guaranteed that each α-cut is a connected region (connected in the sense of Rosenfeld).[2]

After segmentation, a knowledge base containing fuzzy descriptions of the known brain structures is used to identify the structures found in the image. If no secure classification of the structure is possible, then a neural network—trained with different outlines of the known structures—is used to try to make the identification. If no classification is possible, a fuzzy rule-based system is used to adopt the parameters used for the segmentation step. Then, the segmentation restarts with this new parameter values. If there is still no classification possible, the structure will be classified as unknown.[1,2]

A programming language has been developed for use in soft-computing methods for medical image processing. This language supports the user with several hundred commands and the ability to use fuzzy descriptions, fuzzy data bases and fuzzy knowledge bases. Also, neural networks, genetic algorithms and evolutionary strategies are supported: these could be used to allow parallel optimization of the various parameters. Distribution of processing task is done by automatic load balancing.

The main tasks that demand high computing power are the selection and optimization of knowledge-bases or KBs (here the KBs are those of each individual), and these are distributed to several processors for parallel computing. (Clearly, the reason of parallelization is to reduce computation time.) Our concept, based on evolutionary algorithms (EA) offers the ability to distribute the individual knowledge bases on different processors for the calculation of the fitness function (balance).

EAs form a class of probabilistic optimization technique motivated by the observation of biological systems. Although these algorithms are only crude simplifications of real biological processes, they have proved to be very robust and due to their parallel nature and efficient implementation. The basic idea of evolutionary algorithms involves the use of a finite population of individuals (KBs). We found out that the choice of best fitness function (balancing) and the ability to process many generations to make the result more efficient, especially important in this complex field of image analysis.

Madjid Fathi
NASA ACE Center
UNM-EECE Building Rm. 134
Albuquerque, NM 87131, USA
E-mail: fathi@eece.unm.edu

Jens Hiltner
UNI-Dortmund, OH 16, LS1
44221 Dortmund
Germany

References

1. M. Fathi and J. Hiltner, *Using Iconic Fuzzy Sets for Object Classification,* **Proc. EUFIT '98,** pp. 1316-1319, Aachen, Germany, 7-10 September 1998
2. J. Hiltner, M. Fathi, and B. Reusch, *An Approach to use Linguistic and Model based Fuzzy Expert Knowledge for the analysis of MRT Images,* **Int'l J. on Image and Vision Computing 19** (4), pp. 195-206, March 2001.
3. W. Menhardt, **Unscharfe Mengen (Fuzzy Stes) zur Behandlung von Unsicherheit in der Bildanalyse,** Doctoral-Thesis (in German), Uni-Hamburg, Germany, 1990.
4. A. Rosenfeld, *Fuzzy Digital Topology,* **Information and Control 40,** pp. 76-87, 1979.

The uniqueness of the color of human skin

In the field of computer science, one of the major motivations behind understanding the appearance of human skin is the realistic rendering and automatic location and identification of people from color images. There is a substantial body of work in this area that relies on conventional tri-color Red-Green-Blue (RGB) sensor data[1] and on chroma-model based approaches.[2] RGB data is prevalent, easy to collect and mimics human color sensitivity. It is therefore a natural and practical approach to use it in investigating skin recognition and rendering. The drawback of RGB-based methodologies is that they cannot capture the variations that we perceive in human skin. The color and shading of skin is affected by, among other things, changes in lighting, temperature, emotional state, exposure to different environmental conditions, and race. To improve the existing techniques for the realistic rendering of people, and for automatic human detection, we must isolate the effects of each of these factors and understand how each of them affect the appearance of skin. RGB data does not provide sufficient amount of detail to allow for this type of analysis.

A better understanding of skin reflectance can be achieved through spectrographic analysis. For this work, we used the radiometric facility of the General Robotics Automation and Sensory Perception laboratory of the University of Pennsylvania. We measured the light reflected from the skin using a high-resolution, high-accuracy spectrograph under precisely calibrated illumination conditions. The dense spectral measurements that we obtained allowed us to formulate a biological explanation of skin color and its variations. They also enabled us to discriminate between human skin and dyes designed to mimic human skin color.

We measured the skin reflectance of 23 volunteers ranging from 20 to 40 years old. Out of the 23 volunteers, 18 were male and five female. We tried to get a diverse collection of skin tones: 16 of our subjects were Caucasian, three were Asian, two of African descent and two were Indian. Two different samples were taken for each subject: one for the back of their hand and one for the palm, with the light falling approximately on the center of the hand. The final measurement was the ratio of the light reflected from the skin over the light that was incident on the skin.

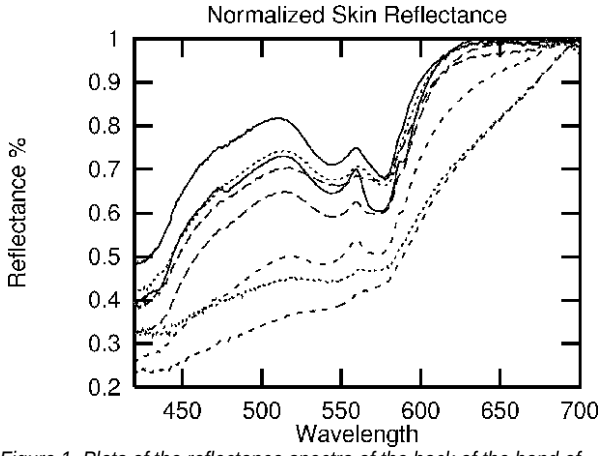

Figure 1. Plots of the reflectance spectra of the back of the hand of various subjects.

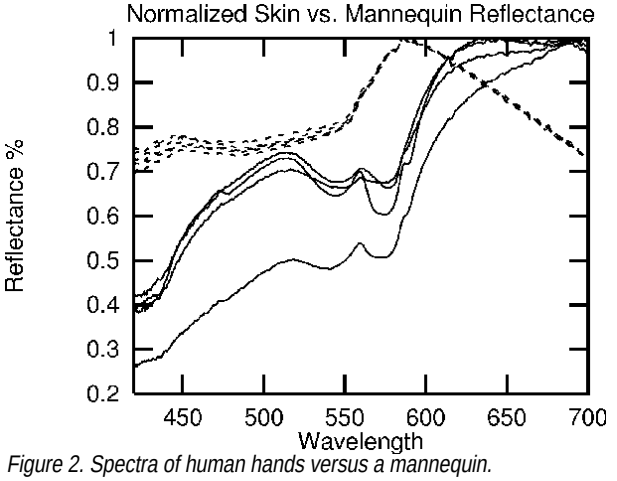

Figure 2. Spectra of human hands versus a mannequin.

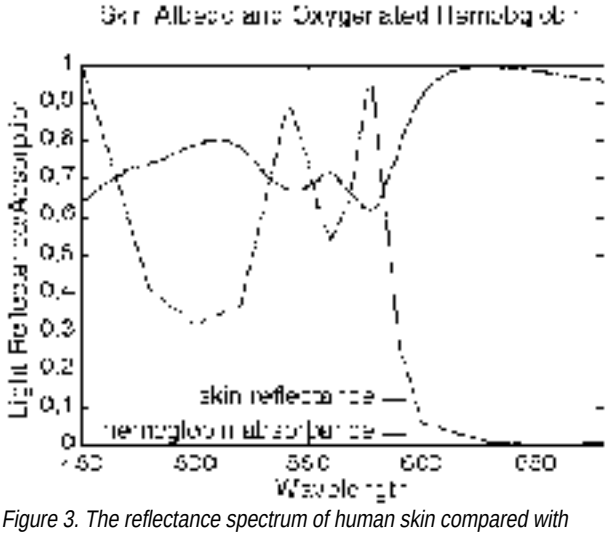

Figure 3. The reflectance spectrum of human skin compared with the absorption spectrum of oxygenated hemoglobin.

Our measurements showed that, overall, the percentage of light that was reflected from human skin increased with wavelength. Around 575nm there was a specific shape that looks like the letter W (two dips with a bump in the middle). Detailed analysis of the collected data revealed that for 90% of the subjects the first local minima of the W occurred at 546nm on average, the local maximum occurred at 559nm on average and the 2nd local maxima occurred at 576nm on average (see Figure 1). The remaining 10% were subjects with very dark shaded skin belonging to no distinct race. The hands of these people (not their palms) reflected a smaller proportion of the incident light (which is how a darker surface can be described) and did not exhibit the W pattern of the other plots.

The next question that arose was whether this pattern is sufficiently unique to provide for the identification of human skin, especially when compared to a mannequin that carries the same key features as humans (lips, nose, eyes, arms, legs etc.). We took five measurements of the spectrum of light reflected by a mannequin. The spectrographic measurements clearly show that the color of the mannequin is quite distinct from that of real skin, although it is designed to mimic it (see Figure 2).

The existence of the W pattern only in the human skin lead us to believe that it can be linked to the physics of skin reflectance and can thus become a valid cue for reliable skin recognition (capable of discriminating materials designed to mimic the color of human skin, and aid in more realistic modeling and rendering.

A closer look at the various chromophores in the skin and their absorption spectra provided the biological explanation we were hoping for. The light absorption in the outer layers of the skin is typically dominated by the absorption caused by melanin. The absorption spectrum of melanin is roughly monotonically decreasing as wavelength increases. The inner layers of the skin are heavily permeated with blood vessels that contain oxygenated hemoglobin, HbO_2. The absorption spectrum of HbO_2 exhibits the inverse W pattern (i.e. an M pattern) located at almost identical to the wavelengths (i.e. 542nm, 560nm and 576nm respectively).[3] This indicates that the oxygenated hemoglobin in the blood vessels is responsible for the skin's W pattern. Heavily pigmented skin has increased amounts of melanin which absorbs most of the light, allowing a much smaller percentage of the incident light to reach the vasculature of the skin. Thus the hemoglobin absorption bands, although still present, are not de-

continued on p. 9

Three-dimensional measurement for industrial applications

Numerous industrial applications require the highly-accurate measurement of free-form objects in various settings. In the automotive industry, for example, these measurements can be intended for design, body-assembly of engineering prototypes, reverse engineering, quality control of parts, assembly in production, measurement within assembly lines and final quality assurance. New market requirements such as a larger number of new car models, a shorter life term of each model, and shorter time-to-market require quick ramp-up times and engineering processes, increased production flexibility, and smaller production batches.

For these purposes, various techniques and methods of 3D part measurement have been introduced and employed in industrial environments over the years. Traditional non-contact optical methods include using light structured with Moire patterns, laser trackers and photogrammetry. These techniques generally achieve higher throughput than most non-optical methods: as well as lower accuracy rates that are not generally acceptable. Solutions based on laser trackers—where reflective hemispheres are operator-scanned around a feature to reflect a laser beam back to a measuring device—achieve higher accuracy on some surface types, but are operator dependent. They require many types of attachment per type of feature, do not produce dense enough data, and are essentially contact-based. Structured light techniques require multiple sequential snapshots, thus limiting them to applications in which time-varying changes are minimal. Photogrammetry systems, specifically those that require the placement of special targets or markers on the measured parts, can achieve very high accuracy levels. However, they can only be used for measuring specific target points. They are not suitable for dense surface scanning, and usually require intense manual intervention by the operators.

Here we discuss a technology that combines the high-speed data acquisition provided by high-resolution CCD cameras with indirect photogrammetry (where targets are placed in fixed locations in the background) and sophisticated 3D reconstruction algorithms (an extended version of the paper with more details can be found in Reference 1). This is possible because we have the ability to detect and measure the targets accurately, acquire images of the object, reconstruct them quickly and accurately, and stitch tiles together (integrate many smaller fields of view into one large one). In addition, the technology is robust and enables the measurement of untreated shiny metallic and plastic parts under different working environments, including factory shop floors. These features have been combined together at CogniTens Ltd., a company that supplies non-contact 3D measurement systems for the industrial metrology market.

Figure 1. The Optigo™ 100 3D measurement system.

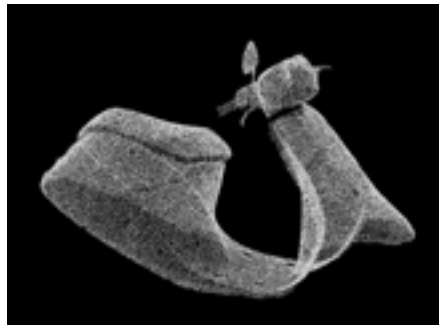

Figure 2. A cloud of points representing the 3D structure of a scooter, as measured by an Optigo™ system.

Reconstruction of 3D shape

The reconstruction process is based on the structure-from-motion principle of extracting 3D shape from multiple 2D projections using a pinhole camera model (3D-from-2D geometry). In a nutshell, given two or more views of a set of 3D features, the corresponding 2D features are first brought into correspondence, then the relative locations of the camera are recovered from these matches, and finally the location of the 3D features are recovered by triangulation. In other words, the inversion process—going from 2D feature locations across multiple views to the corresponding 3D feature locations—requires two basic ingredients. The first of these is the ability to accurately locate image features from the local brightness distribution of each image and accurately match those features across multiple images together, referred to as the correspondence process. The second is the ability to extract the relative locations of the cameras from the matching 2D points.

The challenges in this process are two-fold. First, the correspondence process is constrained by the geometry because the images are not arbitrary but are produced from the same 3D object. Therefore the correspondence process is best approached by combining photometric principles—modeling the change of brightness distribution across images—and geometric constraints. Second, the relative camera locations are governed by two families of parameters: the internal parameters describing the focal length, location of principle point, and skew of local coordinate system;

continued on p. 9

Image analysis for the food industry: Digital color camera photographs and nuclear magnetic resonance images

Meat consumers expectations of quality are constantly growing. This is forcing the adoption of increasingly strict quality control measures and, as a result, the meat industry is looking for new methods of meat quality evaluation. In addition, researchers want improved techniques to deepen their understanding of meat "features". Fat content in meat is one element that influences some important meat quality parameters and has been shown to influence palatability characteristics. Though there are several ways of analyzing quantitative fat content and its visual appearance in meat, few of them are fully adequate. For instance, chemical analysis is currently used to determine intramuscular fat content in beef, but it requires large amounts of organic solvents.

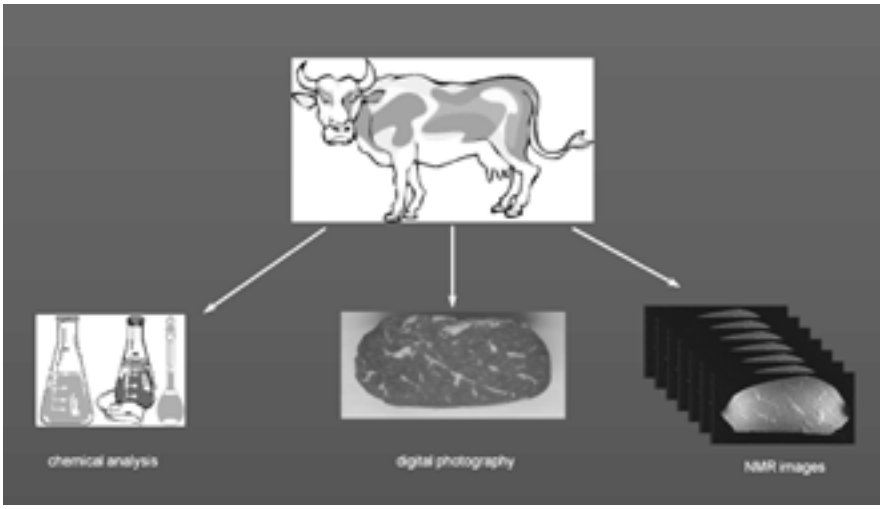

Figure 1. Methods to analyze fat content in meat.

Recent advances in the area of computer and video processing have created new ways to monitor quality in the food industry. (An overview of these methods is shown in Figure 1.) Image processing methods have been successfully applied to meat images in order to determine the percentage and the distribution of various substances. Specifically, we have been working with camera photographs and magnetic resonance images of meat. Segmentation algorithms have been optimized for these kinds of images in order to classify different substances as muscle, fat and connective tissue.

Color images of beef M. longissimus dorsi were captured by a Sony DCS-D700 camera. The same exposure and focal distance were used for all images. The meat pieces were lit with two lamps, each with two fluorescent tubes (15W). Polaroid filters were used on the lamps and on the camera to avoid specular reflections. Images were 1344×1024 pixel matrices with a resolution of 0.13×0.13mm. All these images were analyzed for fat percentage and distribution. In order to measure fat percentage a segmentation algorithm has been optimized for these kinds of images.[1] The method is based on the substance characteristics in the three-dimensional color space (RBG) and on the intrinsic fuzzy nature of these structures, where pixels could belong to multiple classes with varying degrees of certainty. The method is fully automatic and combines a fuzzy clustering algorithm, the fuzzy c-means algorithm, and a genetic algorithm (an optimization technique inspired by natural evolution). The percentage of various substances within the sample are determined; the number, size distribution, and spatial distribution of the extracted fat "spots" (that are impossible to measure by chemical analysis) are measured by image analysis with high accuracy.[1] Our results show that image analysis is a powerful method of quantifing the visual appearance of fat in meat.

We also investigate the use of a new technology to control the quality of food: nuclear magnetic resonance (NMR) imaging. The NMR technique has been developed and greatly improved for medical imaging and is in common clinical use. We believe that NMR imaging has a future application in the field of food science, which—in combination with image processing techniques—can lead to automatic and quantitative methods of assessing meat quality. The inherent advantages of NMR images are many. Chief among these are unprecedented contrasts between the various structures present in meat: muscle, fat, and connective tissue. In particular, connective tissue and fat, which are almost indistinguishable in color images taken by a camera, contrast highly in NMR images, i.e. fat areas are lighter, while connective tissue is darker than other structures. In addition, NMR imaging allows a 3D analysis of the meat composition, so the volumetric content of fat—not just the fat that is superficially visible—can be readily measured.

The segmentation algorithms used for Magnetic Resonance images also include a filtering technique to remove intensity inhomogeneities caused by non-uniformities in the magnetic fields during acquisition. A good correlation (r=0.77, p=0.02) was obtained between the mean fat content (measured by chemical analysis) and by the present method. This value was better than the correlation value we obtained between chemical analysis and image analysis applied to digital photographs of the same meat samples, probably because NMR imaging provided the three dimensional structure of the meat samples based on the chemical information of the proton mobility and distribution.[2] We also developed a method of describing and quantifing the distribution of fat, and we have applied it to both camera pictures and NMR images.[3] The NMR technique has proved to be a powerful tool in measuring fat content non-destructively, non-invasively and continuously.

Lucia Ballerini
Centre for Image Analysis
Lägerhyddvägen 17
752 37 Uppsala, Sweden
E-mail: lucia@cb.uu.se
http://www.cb.uu.se/~lucia

References

1. L. Ballerini et al., *Colour image analysis technique for measuring of fat in meat: An application for the Meat industry,* **Proc. SPIE 4115,** 2001.
2. L. Ballerini et al., *Testing MRI and Image Analysis Techniques for Fat Quantification in Meat Science,* **Proc. IEEE Nuclear Science Symp. and Medical Imaging Conf.,** Lyon, France, October 2000
3. L. Ballerini, *A Simple Method to Measure Homogeneity of Fat Distribution in Meat,* **Proc. 12th Scandinavian Conf. on Image Analysis,** Bergen, Norway, June, 2001

A psychophysically-based model of glossy surface appearance

continued from cover

shown in Figure 1. The figure shows that, under our test conditions, apparent gloss has two dimensions related to the contrast of the reflected image *(c)* and the sharpness or distinctness of the reflected image *(d)*.

In the second experiment, we used magnitude estimation to place metrics on these dimensions. Subjects viewed single images from the stimulus set and rated how glossy the objects appeared. We analyzed these ratings with regression techniques to derive metrics for the dimensions that relate changes in apparent gloss to variations in the physical properties of the surfaces:

$$c = \sqrt[3]{\rho_s + \rho_d/2} - \sqrt[3]{\rho_d/2}$$

$$d = 1 - \alpha$$

We used these metrics to rewrite the parameters of the physically-based Ward light reflection model in perceptual terms. The result is a new psychophysically-based light reflection model that relates the physical dimensions of glossy reflectance and the perceptual dimensions of glossy appearance. The following sections demonstrate how the new model can be used to describe and control the appearance of glossy surfaces.

Gloss matching

Many studies have noted that apparent gloss is affected by a surface's diffuse reflectance. This effect is illustrated in the top row of Figure 2 where the white, gray, and black objects have the same physical gloss parameters (rs = 0.099, a = 0.04), but the lighter ones appear less glossy than the darker ones. This phenomenon makes it hard to create light and dark surfaces that have the same apparent gloss. The bottom row of Figure 2 shows the results produced with our new model. Here the objects have been given the same visual gloss parameters (c = 0.057, d = 0.96), and they appear similar in gloss despite their lightness differences. Using the parameters provided by the new model should make it much easier to create objects that match in apparent gloss.

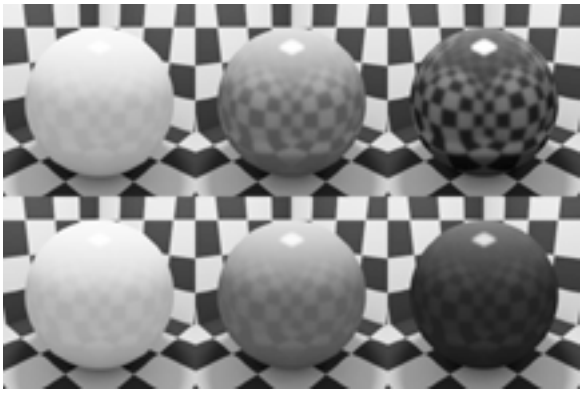

Figure 2. Matching apparent gloss: white, grey, and black objects having the same physical gloss parameters (top row) and visual gloss parameters (bottom row).

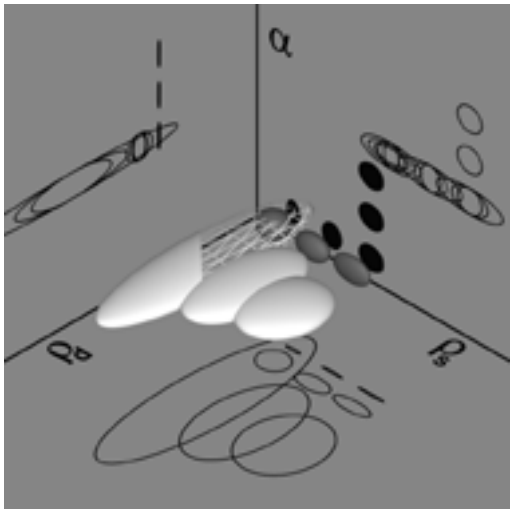

Figure 3. Just noticeable differences in gloss: the ellipsoids indicate the changes in material properties required to produce visible differences in gloss for the surfaces defined by the three parameters.

Just noticeable differences in gloss

Just noticeable difference (JND) metrics can be used to predict acceptable tolerances in measurement and manufacturing processes. We have attempted to estimate JNDs in gloss for a subset of the surfaces we tested. Figure 3 shows these JND values plotted in terms of the physical parameters of the Ward model. The ellipsoids indicate the changes in material properties required to produce visible changes in gloss for each of the surfaces. There are several things to notice: lighter surfaces (high rd) require larger changes than darker ones (low rd) to produce JNDs; increasing rs reduces the size of a JND more for lighter surfaces than for darker ones; and a has little effect on JNDs over the range of surfaces we tested. These results may lead to new methods for establishing visual tolerances in the measurement and manufacturing of glossy materials.

In many ways, this work parallels early studies done to establish the science of colorimetry. We hope it inspires further research toward developing psychophysical models of the goniometric properties of surface appearance to complement widely-used colorimetric models.

James A. Ferwerda
Program of Computer Graphics
580 Rhodes Hall
Cornell University
Ithaca, NY 14853
E-mail: jaf@graphics.cornell.edu
http://www.graphics.cornell.edu/~jaf

References

1. F. Pellacini, J.A. Ferwerda, and D.P. Greenberg, *Toward a psychophysically-based light reflection model for image synthesis*, **Proc. SIGGRAPH 2000,** pp. 5564, August 2000.
2. J.A. Ferwerda, F. Pellacini, and D.P. Greenberg, *A psychophysically-based model of surface gloss perception*, **Proc. SPIE 4299,** 2001.

Human color constancy: model and performance

continued from p. 3

dominant color towards the achromatic reference point, representing a CC correction. The inclination towards the corrected reference (open circles of "white" illumination), rather than the reference itself (solid circle of "white" illumination) demonstrates the algorithm's human vision performance. Similar results were obtained in cases where the scene was illuminated with multiple chromatic illumination sources.

Hedva Spitzer and **Sarit Semo**
Department of Biomedical Engineering
Faculty of Engineering, Tel Aviv University
Tel Aviv, Israel
E-mail: {hedva, sarits}@eng.tau.ac.il

Reference

1. H. Spitzer and S. Semo, *Color Constancy: A Biological Model and its Application for Still and Video Images*, **Pattern Recognition,** *special issue on Color, in press.*

Three-dimensional measurement

continued from p. 6

and the external parameters describing the rotation and translation in 3D space between the camera coordinate systems. Taken together, this leads to a nonlinear relation between 2D matching points and 3D coordinates.

The approach taken in our case is to first describe the 3D-from-2D problem in projective space in which structure is defined relative to some virtual plane. The projective approach allows the combination of the two families of parameters into one set that can be recovered linearly in a straightforward manner. This approach is referred to as a relative affine framework and enables the acquisition of useful 3D information without any form of internal camera calibration. The linearity of the process also ensures a unique and stable solution and is a key factor in allowing the automation of the measurement process.

The geometric and algebraic constraints of the 3D-from-2D problem, including the combination with photometric constraints, is described by a unique family of multilinear forms whose coefficients form a tensor, known as the "tri-linear tensor". One of the key features of the tensor is that it describes the 3D-from-2D constraints under all possible situations—that is, it is not subject to any form of singularity—thereby elevating the numerical stability of the measurement process by an order of magnitude in some typical scenarios. These include situations where the camera motion is linear[2,3] or where objects' local geometry approximate second-order surfaces. Furthermore, the tensor is a key factor in combining the photometric and geometric constraints, thus giving rise to a very tight cycle of correspondence and reconstruction and thereby further elevating the accuracy levels and the automation of the process.

The technology described was brought together into one platform, the Optigo™ system (see Figure 1), which provides high-accuracy, portable, 3D measurement capabilities. The technology does not require prior calibration of the system and enables accurate measurement even in difficult industrial environments. Optigo™ systems are based on a measurement head that includes three high-resolution CCD cameras, enabling the capture of large areas. The acquisition time of the system is less than a second, reducing sensitivity to vibrations that may exist in industrial conditions. Measurement is achieved by aiming the optical head at the desired area: 3D measurements are then made on the basis of 2D images acquired. The measurements that can be taken include the acquisition of highly dense coordinates on the object surface (see, for example, Figure 2), cross-sections, measurement of features such as holes and slots, as well as object edges. Enhanced capabilities allow comparison of measurement data to their CAD model and visual display of differences and visualization feedback for manufacturing process control.

Ron Gershon
CogniTens Ltd.
PO Box 1713
47282 Ramat Hasharon
Israel
Phone: +972 3 548-8210
Fax: +972 3 547-2224
E-mail: ron@cognitens.com
http://www.cognitens.com

References

1. R. Gershon, M. Benady, and T. Shalom, *3D Reconstruction from multiple 2D views using tri-linear tensor technology,* **SPIE Proc. 4298,** 2001.
2. A. Shashua, *Algebraic functions for recognition,* **IEEE Trans. on Pattern Recognition and Machine Intelligence 17** (8), pp. 779-789, 1995.
3. A. Shashua and N. Navab, *Relative affine structure: canonical model for 3D from 2D geometry and applications,* **IEEE Trans. on Pattern Analysis and Machine Intelligence 18** (9), pp. 873-883, 1996.

The uniqueness of the color of human skin

continued from p. 5

tectable.

Elli Angelopoulou
Computer Science Department
Stevens Institute of Technology
Castle Point on Hudson
Hoboken, NJ 07030
E-mail: elli@cs.stevens-tech.edu

References

1. M.M. Fleck, D.A. Forsyth, and C. Bregler, *Finding Naked People,* **Proc. European Conf. on Computer Vision and Pattern Recognition 1996**, pp. 593-602, 1996.
2. S. Inokuchi, H. Nakai, and Y. Manabe, *Simulation and Analysis of Spectral Distributions of Human Skin,* **Proc. Int'l Conf. on Pattern Recognition 1998**, pp. 1065-1067, 1998.
3. W.G. Zijlstra, A. Buursma, and W.P. Meeuwsen-van der Roest, *Absorption Spectra of Human Fetal and Adult Oxyhemoglobin, De-oxyhemoglobin, Carboxyhemoglobin, and Methemoglobin,* **Clinical Chemistry 37** (9), pp. 1633-1638, 1991.

Circular dynamic stereo system

continued from p. 2

further away. Each frame has three-dimensional information about the tracer particles, and the velocity distribution can be obtained by analyzing consecutive frames. Figure 3 shows the result of this analysis.

The second example is the measurement of a water surface in a tank. Aluminum powder (20μm) is strewn over the surface of the water. This powder forms a thin film that moves with any waves that occur. Multi laser spots (30mW) are projected onto the surface and are reflected by the aluminum powder. Figure 4 shows a recorded image of multi laser spots using a circular dynamic stereo system. Information, such as the size and position of each streak on the image, is converted to 3D position data for each laser spot, and the water surface is thereby reconstructed and can be displayed (see Figure 5).

Using our system, 3D information about multiple points can be recorded in a single image at a given instant, and this information can be extracted by processing the image. The novelty of our system lies in the fact that it allows 3D measurement of moving objects and those are otherwise unstable.

Kikuhito Kawasue
Faculty of Engineering
Miyazaki University
Gakuen Kibanadai Nishi
Miyazaki, 889-2192 JAPAN
E-mail: kawasue@computer.org

Yuichiro Ohya
West Japan Fluid Engineering Laboratory
339-37 Kitamatsuragun, Kosasa
Nagasaki, 857-0401 Japan
E-mail: fel_oya@mx9.freecom.ne.jp

Takakazu Ishimatsu
Faculty of Engineering
Nagasaki University
14-1 Bunkyou
Nagasaki, 857-11 Japan
E-mail: ishi@net.nagasaki-u.ac.jp

References

1. K. Kawasue and T. Ishimatsu, *3D measurement of moving particles by circular image shifting,* **IEEE Trans. on Industrial Electronics 44** (5), pp. 703-706, October 1997.
2. K. Kawasue, O. Shiku, and T. Ishimatsu, *Range finder using circular dynamic stereo,* **Proc. Int'l Conf. on Pattern Recognition,** pp. 774-776, 1998.

Total multispectral imaging

continued from p. 12

stimuli of all reproduced colors differ from the original.

A multispectral imaging system as described below solves all these fundamental problems by capturing the complete spectral light stimuli in all the pixels of an image and reproducing an approximation to these original spectral stimuli by multichannel image reproduction (see Figure 2). The so-called "multispectral camera" developed in our laboratory captures an image via 16 narrow band spectral filters. These are moved sequentially in front of a B&W-CCD camera by a fast mechanical switch to capture 16 spectral separations of an image at 12 bits of resolution (a camera with only eight filters is shown in Figure 2 for simplicity).[4] The 16 separations provide a discrete scan of the spectral light stimulus in each of the 2000×2000 pixels of the image. Before starting the capture of an image, the scan of a white reference is taken and the scanned values of the actual image are afterwards normalized by the white reference values.

The output of the camera thus delivers the spectral scan of an image referenced to illuminant E, the equal energy distribution of light. This makes the system independent of the light source on one hand and, on the other, allows for the introduction of any other light source with its spectral power distribution for reproduction later (by multiplication of the respective spectra). The multispectral camera thus allows the capture of color information without systematic errors and, in fact, smallest color errors yet are practically achieved using the developed device. Experimental errors are <0.25 units of CIE DE94. The capture of an image takes approximately 30s at present.

A six-channel display is under development as a first step. This is realized by two digitally-controlled cameras equipped with six narrow-band spectral filters. The six channels are controlled by the signals of the multispectral camera via an optimized mathematical algorithm. This allows for the reproduction of colors with small reproduction errors for different observers and, moreover, a larger volume of colors can be reproduced compared to conventional three-channel displays. Even with this system of only six channels, color reproduction errors for all the 24 observers characterized in Figure 1 are below 1.4 CIE DE94 units compared to values of at least 8-10 CIE ΔE94 units in conventional systems.

The amount of data to be handled and transmitted from a multispectral camera to the display is, of course, much higher than in conventional tristimulus color systems. Therefore, efficient data encoding algorithms have been developed to reduce the amount of data as far as possible without losing the required quality.[5]

First products of the multispectral technology are offered by "Color Aixperts" in Aachen, Germany. Even when using the multispectral camera for image capture and reproducing images on a conventional cathode ray tube, remarkable improvement in color quality is achieved because all systematic errors inherent in conventional three-channel cameras are completely avoided. Apart from the reproduction on multi-channel displays, printing of images captured by the multispectral camera also improves color quality because the features of a printer can be optimized better if the exact spectral information of the colors is available at the input. Multichannel printing with six or more printing colors is also under investigation for future systems.

Bernhard Hill
Aachen University of Technology
E-mail: hill@ite.rwth-aachen.de

References

1. B. Hill, *Color capture, color management and the problem of metamerism,* **Proc. SPIE 3963,** pp. 3-14, 2000.
2. B. Hill, *Aspects of total multispectral image reproduction systems,* Proc. 2nd Int'l Symp. on High Accurate Color Reproduction and Multispectral Imaging, Chiba University, Japan, October 2000.
3. G. Wyszecki and W.S. Stiles, **Color Science,** John Wiley & Sons, Inc, New York, 1976.
4. F. König and W. Praefcke, *A multispectral scanner,* **Proc. CIM 98 Color Imaging in Multimedia,** Derby, UK, 1998, and **Color Imaging, Vision and Technology,** John Wiley & Sons Ltd, 1999.
5. F. König and W. Praefcke, *Multispectral Image Encoding,* **ICIP,** Kobe, Japan, 1999.

CALENDAR

2001

SID Symposium 2001
3-8 June
San Jose, California USA
Contact: Society for Information Display, 1526 Brookhollow Dr., Ste. 82, Santa Ana, CA 92705-5421 USA. Phone: (1) 714/545-1526. Fax: (1) 714/545-1547. E-mail: socforinfodisplay@mcimail.com. Web: www.sid.org

AIC Color 01: The 9th Congress of the International Color Association
24-29 June
Rochester Riverside Convention Center
Rochester, New York
SPIE to publish Proceedings. Contact Congress Secretariat: Ms.Cynthia Sturke, Email:iscc@compuserve.com Web: www.iscc.org/aic2001. SPIE is publishing the Proceedings

Optical Science and Technology SPIE's Annual Meeting
29 July - 3 August
San Diego Convention Center
San Diego, California, USA
Technical Exhibit: 31 July-2 August.

2nd International Symposium on Multispectral Image Processing and Pattern Recognition
22-24 October
Wuhan, China
Sponsored by Huazhong Univ. of Science & Technology and SPIE.

Integrated Computational Imaging Systems (ICIS)
4-8 November
Albuquerque, New Mexico USA
Sponsored by OSA. SPIE is a cooperating organization. 0Contact OSA's Customer Service: Optical Society of America, 2010 Massachusetts Ave, NW, Washington, DC 20036-1023. Fax: 202-416-6140. E-mail: cust.serv@osa.org. Web: www.osa.org/mtg_conf.

2002

Photonics West
18-25 January
San Jose Convention Center
San Jose, California USA
Including international symposia on
- **LASE '02—High-Power Lasers and Applications**
- **OPTOELECTRONICS '02—Integrated Devices and Applications**
- **BiOS '02—International Biomedical Optics Symposium**
- **SPIE/IS&T's EI '02—Electronic Imaging: Science and Technology**

Education Program and Short Courses; Technical Exhibit.

SID Symposium 2002
19-24 May
Boston, Massachusetts USA
Contact: Society for Information Display, 1526 Brookhollow Dr., Ste. 82, Santa Ana, CA 92705-5421 USA. Phone: (1) 714/545-1526. Fax: (1) 714/545-1547. E-mail: socforinfodisplay@mcimail.com. Web: www.sid.org

Join the SPIE/IS&T Technical Group

...and receive this newsletter

This newsletter is produced twice yearly and is available only as a benefit of membership in the SPIE/IS&T Electronic Imaging Technical Group.

IS&T—The Society for Imaging Science and Technology has joined with SPIE to form a technical group structure that provides a worldwide communication network and is advantageous to the memberships.

Join the Electronic Imaging Technical Group for US$30. Technical Group members receive these benefits:

- *Electronic Imaging* Newsletter
- SPIE's monthly publication, *oe magazine*
- annual list of Electronic Imaging Technical Group members
- discounts on registration fees for IS&T and SPIE meetings and on books and other selected publications related to electronic imaging.

Persons who are already members of IS&T or SPIE are invited to join the Electronic Imaging Technical Group for the reduced member fee of US$15.

Please Print ☐ Prof. ☐ Dr. ☐ Mr. ☐ Miss ☐ Mrs. ☐ Ms.

First (Given) Name _____ Middle Initial _____

Last (Family) Name _____

Position _____

Business Affiliation _____

Dept./Bldg./Mail Stop/etc. _____

Street Address or P.O. Box _____

City _____ State or Province _____

Zip or Postal Code _____ Country _____

Phone _____ Fax _____

E-mail _____

Technical Group Membership fee is $30/year, or $15/year for full SPIE and IS&T Members.

Amount enclosed for Technical Group membership **$** _____

❑ **I also want to subscribe to IS&T/SPIE's *Journal of Electronic Imaging* (JEI)** **$** _____
(see prices below)

Total $ _____

❑ **Check enclosed.** Payment in U.S. dollars (by draft on a U.S. bank, or international money order) is required. Do not send currency. Transfers from banks must include a copy of the transfer order.

❑ **Charge to my:** ❑ **VISA** ❑ **MasterCard** ❑ **American Express** ❑ **Diners Club** ❑ **Discover**

Account # _____ Expiration date _____

Signature _____
(required for credit card orders)

Reference Code: 2819

JEI 2001 subscription rates (4 issues):	**U.S.**	**Non-U.S.**
Individual SPIE or IS&T member	$ 50	$ 50
Individual nonmember and institutions	$225	$245

Your subscription begins with the first issue of the year. Subscriptions are entered on a calendar-year basis. Orders received after 1 September 2001 will begin January 2002 unless a 2001 subscription is specified.

Send this form (or photocopy) to:
SPIE • P.O. Box 10
Bellingham, WA 98227-0010 USA
Phone: (1) 360/676-3290
Fax: (1) 360/647-1445
E-mail: membership@spie.org

Please send me:
☐ **Information about full SPIE membership**
☐ **Information about full IS&T membership**
☐ **Information about other SPIE technical groups**
☐ **FREE technical publications catalog**

Electronic Imaging

The *Electronic Imaging* newsletter is published by SPIE—The International Society for Optical Engineering and IS&T—The Society for Imaging Science and Technology. The newsletter is the official publication of the International Technical Group on Electronic Imaging.

Editor / Technical Group Chair	Arthur Weeks
Technical Editor	Sunny Bains
Managing Editor / Graphics	Linda DeLano
Advertising Sales	Roy Overstreet

Articles in this newsletter do not necessarily constitute endorsement or the opinions of the editors, SPIE, or IS&T. Advertising and copy are subject to acceptance by the editors.

SPIE is an international technical society dedicated to advancing engineering, scientific, and commercial applications of optical, photonic, imaging, electronic, and optoelectronic technologies.

IS&T is an international nonprofit society whose goal is to keep members aware of the latest scientific and technological developments in the fields of imaging through conferences, journals and other publications.

SPIE—The International Society for Optical Engineering, P.O. Box 10, Bellingham, WA 98227-0010 USA. Phone: (1) 360/676-3290. Fax: (1) 360/647-1445. E-mail: spie@spie.org.

IS&T—The Society for Imaging Science and Technology, 7003 Kilworth Lane, Springfield, VA 22151 USA. Phone: (1) 703/642-9090. Fax: (1) 703/642-9094.

Want it published?

Submit work, information, or announcements for publication in future issues of this newsletter by e-mail to Sunny Bains. For full submission information, length and format required, deadline, etc., please go to:

http://www.sunnybains.com/newslet.html.

All materials are subject to approval and may be edited. Please include the name and e-mail address of someone who can answer technical questions. Calendar listings should be sent at least eight months prior to the event.

EIONLINE

New Electronic Imaging Web Discussion Forum launched

You are invited to participate in SPIE's new online discussion forum on Electronic Imaging. The **INFO-EI** mailing list is being "retired" as we move the discussions to the more full-featured web forums. We hope you will participate. To post a message, log in to create a user account. For options see "`subscribe to this forum.`"

You'll find our forums well-designed and easy to use, with many helpful features such as automated email notifications, easy-to-follow "threads," and searchability. There is a full FAQ for more details on how to use the forums.

Main link to the new Electronic Imaging forum: `http://spie.org/app/forums/tech/`

Related questions or suggestions can be sent to `forums@spie.org.`

Total multispectral imaging technology provides high accurate color reproduction

Research at the Technical Electronics Institute of Aachen University of Technology is focused on color and electronic imaging. Fundamental problems of conventional color capture and reproduction and color management are studied as well as multispectral imaging. The largest project, on multispectral imaging,[1,2] is geared towards applications where highly accurate color reproduction is a must. Typical examples are digitization and imaging of textiles, reproduction of the colors of automobiles and furniture, and the archiving of art paintings.

To understand the motivation behind the development of this entirely new color reproduction system, some fundamentals of current color reproduction technology and human color perception should be considered. The basic color stimulus activating the red, green and blue cones in the retina of the human eye is a spectral power distribution of light: either emitted from a light source or reflected from the surface of an object which is being viewed. The three groups of cones of the retina of the human eye collect different parts of this spectral stimulus according to their spectral absorptions or responsivities and generate three primary color signals in the retina. These signals are afterwards processed and transmitted to the brain where they initiate color perception. Typical measured spectral responsivities (called "color-matching functions") of the cones of 24 observers are sketched in Figure 1.[3] They vary from human being to human being, resulting in different primary color signals for each individual. These variations produce one of the fundamental problems of present technology because the conventional optimization of technical color reproduction is based on the color-matching functions of only one observer, the so called CIE 1931 XYZ standard observer. Deviations from this observer have not, up until now, been taken into consideration in our color systems.

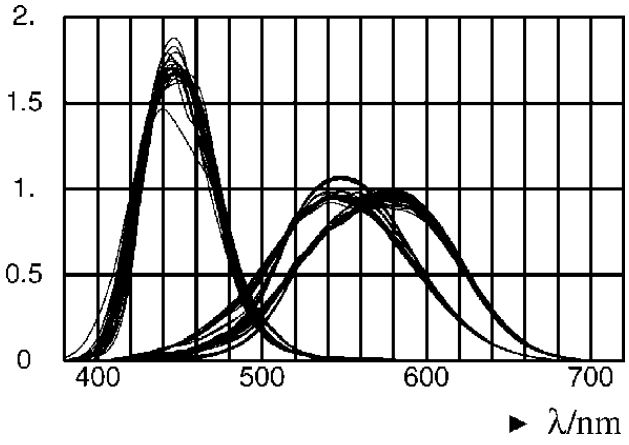

Figure 1. Spectral responsivities (color-matching functions) of the cones of 24 human observers including 2° and 10° observers.

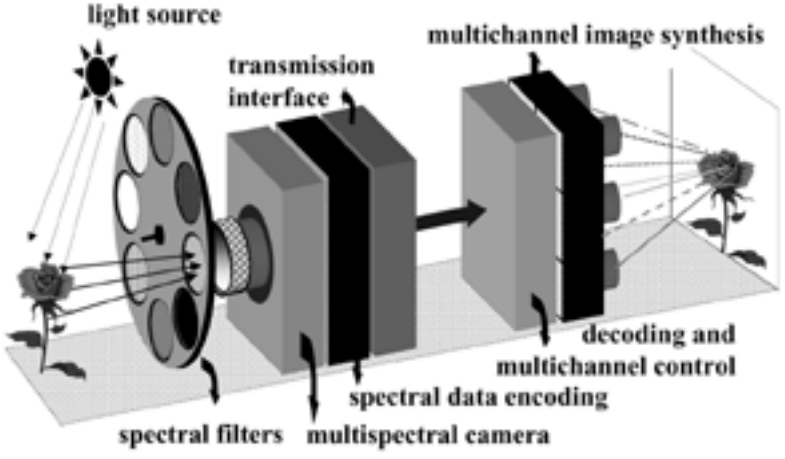

Figure 2. Sketch of a total multispectral imaging system: includes a multispectral B&W-CCD camera and spectral filter wheel, spectral data encoding, open system interface, and a decoding and control unit for multichannel projection-type image synthesis.

Current color-capture devices are based on a three-channel technology considered to approximate human color perception of the standard observer. The three channels of a camera or scanner are therefore equipped with spectral filters, transmitting different parts of a spectral light stimulus in the "red", "green" and "blue" region. Three electronic sensors for each pixel of an image collect the respective transmitted light and produce three output signals. Color analysis of a sensor of that kind would be correct if the overall spectral responsivities of the color channels exactly matched the color-matching functions defined for the standard observer. In practice, this replication of human color vision shows essential disadvantages with respect to the signal-to-noise ratio of electronic color reproduction. Practical color sensors are therefore optimized to achieve the best signal-to-noise ratio rather than matching the standard observer correctly.[1] This causes fundamental errors of color analysis in all our current color imaging systems. In any case, additional errors arise from practical problems of approximating theoretically-optimized spectral responsivities in cameras or scanners.

Another problem in most current systems is caused by the light source used to capture an image or scene. Each light source exhibits its own spectral power distribution that influences the spectral color stimuli and changes the respective human color perception. If the same light source used for image capture is also used for the reproduction, colors will be reproduced best. Yet, in most practical applications, a different light source is used to view a print than for scanning an image. As a result, the

continued on p. 10

SPIE Society of Photo-Optical Instrumentation Engineers

P.O. Box 10 • Bellingham, WA 98227-0010 USA

Change Service Requested

DATED MATERIAL

Non-Profit Org.
U.S. Postage Paid
Society of
Photo-Optical
Instrumentation
Engineers